

Jurnal Kejuruteraan SI 4(1) 2021: 153-160  
[https://doi.org/10.17576/jkukm-2021-si4\(1\)-19](https://doi.org/10.17576/jkukm-2021-si4(1)-19)

## Deformations' Predictions by Utilizing Load Blast Enhanced against Structural Arbitrary Langrangian Eulerian Methodologies: An LS-DYNA Numerical Simulation Study

(Ramalan Deformasi dengan Menggunakan Ledakan Beban yang Ditingkatkan terhadap Kaedah Eulerian Langrangian Arbitrari Struktural: Kajian Simulasi Numerik LS-DYNA)

Mohd Zaid Othman<sup>a,\*</sup>, Tan Kean Sheng<sup>a</sup>, Jestin Jelani<sup>a</sup>, Khairul Hasni Kamarudin<sup>a</sup> & Amir Radzi Ab Ghani<sup>b</sup>

<sup>a</sup>Faculty of Engineering, National Defence University of Malaysia (UPNM), Malaysia

<sup>b</sup>Faculty of Mechanical Engineering, Universiti Teknologi MARA, Shah Alam, Selangor, Malaysia

\*Corresponding author: [zaid002@gmail.com](mailto:zaid002@gmail.com)

Received 17 March 2021, Received in revised form 29 April 2021

Accepted 30 August 2021, Available online 30 September 2021

### ABSTRACT

*Numerical simulation study to predict the transient (maximum) deformation of a rolled homogeneous armor plate which was loaded by the explosion of spherical trinitrotoluene bomb by using the 'load blast enhanced' and 'structured arbitrary langragian eulerian' methodologies in LS-DYNA is reported in this paper. Three numerical simulation models that utilized the 'load blast enhanced' and three numerical simulation models that utilized the 'structured arbitrary langragian eulerian' methodologies in LS-DYNA were produced and their results were used to predict and validate the deformations of three blast experimental tests of rolled homogeneous armor plates obtained from a published paper. This study showed that the numerical simulation results from the 'load blast enhanced' methodology gave better agreement than the 'structured arbitrary langragian eulerian' methodology with an average percentage differences of around 17% for all three cases.*

**Keywords:** Load blast enhanced; structured arbitrary langrangian eulerian; blast loading; numerical simulation; TNT; LS-DYNA

### ABSTRAK

*Kajian simulasi berangka untuk meramalkan ubah bentuk sementara (maksimum) plat perisai homogen bergulung yang dimuatkan oleh letupan bom trinitrotoluena sfera dengan menggunakan metodologi 'beban letupan dipertingkatkan' dan 'struktur rawak langrangian eulerian' di dalam LS-DYNA dilaporkan dalam kertas ini. Tiga model simulasi berangka yang menggunakan 'beban letupan dipertingkatkan' dan tiga model simulasi berangka yang menggunakan metodologi 'struktur rawak langrangian eulerian' di dalam LS-DYNA dihasilkan dan hasilnya digunakan untuk meramalkan dan mengesahkan ubah bentuk tiga ujian eksperimen letupan plat perisai homogen bergulung yang diperolehi daripada kertas yang diterbitkan. Hasil kajian menunjukkan bahawa hasil simulasi berangka dari metodologi 'beban letupan dipertingkatkan' memberi persetujuan yang lebih baik daripada metodologi 'struktur rawak langrangian eulerian' terstruktur dengan perbezaan purata sekitar 17% untuk ketiga-tiga kes.*

**Kata kunci:** Beban beban ditingkatkan; eulerian langrangian rawak berstruktur; pemuatan letupan; simulasi berangka; TNT; LS-DYNA

## INTRODUCTION

Quite recently, a massive accidental explosion occurred at the city of Beirut (Figure 1), Lebanon killing around 200 people, injuring around 5 000 people and around 30 000 people lost their homes (BBC 2020). The huge accidental explosion was caused by the detonation of 2 750 tons of ammonium nitrate that were stored at the port of Beirut since 2013. The fatal shockwave of the explosion travelled in a spherical direction damaging glass buildings as far as 9 km from ground zero. Research publications (Chiquito et al. 2020; Gannon 2019; Huang et al. 2019; Kong et al. 2020; Li et al. 2020; Pratomo et al. 2020; Qin et al. 2020; Su et al. 2021; Wu et al. 2020; Zhu et al. 2020) on the numerical simulations of blast related scenarios are quite vast in the open literature due to the high cost, high level of difficulties, and lots of safety issues in performing real physical experimental blast tests. With the advancement of computational hardware and software technologies, users can now utilize numerical simulations to perform and solve comprehensive and complex engineering problems that integrates structural as well as fluid interactions in their analysis (Faucher et al. 2019; Hughes et al. 2013; Nguyen & Gatzhammer 2015; Spinosa & Iafrati 2021; Yu & Jeong 2016; Yuan et al. 2017).



FIGURE 1. The aftermath of the city of Beirut, Lebanon after a huge explosion that occurred on 4th August 2020 due to the accidental detonation of 2,750 tons of ammonium nitrate chemical compound

Source: BBC (2020)

The objective of this paper is to utilize numerical simulation analysis software (LS-DYNA 2020) in order to predict three transient deformation results of performed experimental blast tests from a published paper (Neuberger et al. 2009). Neuberger et al. (2009) performed three experimental spherical trinitrotoluene (TNT) bomb tests that were situated on top of circular rolled homogeneous armor (RHA) plates by varying the masses of the TNT bombs and standoff distances of the TNT bombs with the

top surfaces of the RHA plates. They performed three experimental blast tests in order to investigate and acquire the maximum transient deformations (that had greater magnitude as compared to its final deformation) experienced by the RHA plate in the very early stages of the blast loading before it vibrates and achieved its final deformations. Two methods of numerical simulation analyses (LS-DYNA 2020) utilizing the ‘load blast enhanced (LBE)’ and ‘structured arbitrary eulerian langrangian (S-ALE)’ technics will be employed in order to predict the maximum transient deformations experienced by the three experimental tests (Neuberger et al. 2009). These numerical simulations predictions will then be compared and discussed against the published experimental tests data.

## METHODOLOGY

### EXPERIMENTAL TEST

Neuberger et al. (2009) conducted three experimental blast tests on an exposed circular RHA plate with a diameter of 1 m. Figure 2 shows a square RHA plate clamped and bolted tightly between two thick clamp plates. A spherical TNT bomb is located right at the center of the RHA plate suspended in air by four wooden pyramid-shaped that acts as temporary support with the whole structure placed on a rigid concrete base. The TNT bomb was then detonated and it deformed the RHA plate underneath. Figure 3 shows the cross-sectional diagram of the experimental test rig in a two-dimensional view. It could be observed that the spherical TNT bomb was placed at the center of the circular RHA plate, all of the thickness of the RHA plates used in the experimental tests were 20 mm, ‘ $\delta T$ ’ is the maximum transient deformation and the value of ‘ $R$ ’ represents the standoff distance i.e., a length between the central point of the spherical TNT bomb and the top surface of the RHA plate. Figure 4 shows the bottom view of the RHA plate after the completion of the blast test that represents the final deformation of the RHA plate. Table 1 shows the mechanical properties of the RHA together with its dynamic mechanical properties to represent the strain rate effects (Cowper-Symonds equation) used in the experimental blast tests. Table 2 shows the three types of different experimental tests with their respective TNT weights and standoff distances and maximum transient deformations that were obtained during the performed blast tests which will be the main values that will be used to compare and validate the numerical simulation predictions obtained by using the LBE and S-ALE methodologies.

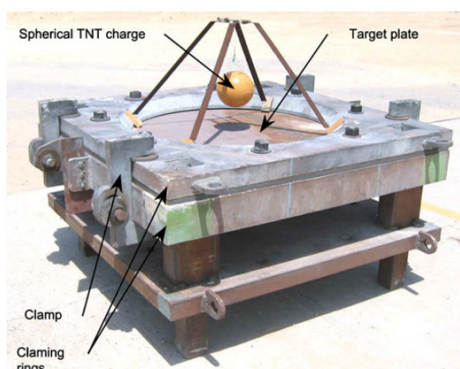


FIGURE 2. The experimental test rig of the fully clamped rolled homogeneous armor steel plate against the spherical TNT explosion

Source: Neuberger et al. (2009)

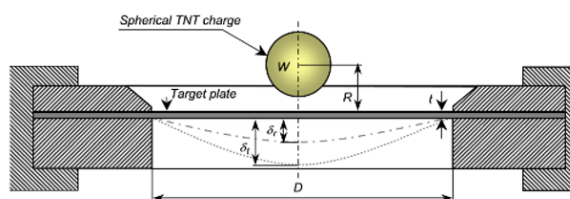


FIGURE 4. The final deformation of the rolled homogeneous armor steel plate for Case 'B', with a standoff distance of 200 mm, 8.75 kg of TNT and 20 mm of plate thickness

Source: Neuberger et al. (2009)

TABLE 1. The mechanical properties of RHA plate

Density ( $\text{kg/m}^3$ )	7860
Young's modulus (GPa)	210
Poisson's ratio	0.28
Strain hardening modulus (GPa)	6.5
Thickness of RHA plate (m)	0.02
Yield strength (MPa)	950
Cowper-Symonds 'C' constant ( $\text{s}^{-1}$ )	300
Cowper-Symonds 'p' constant	5

Source: Neuberger et al. (2009)

TABLE 2. The three different types of experimental tests data with their respective magnitudes of the maximum transient deformations as performed by Neuberger and his co-authors (Neuberger et al., 2009)

Test case	Weight of TNT (kg)	Standoff distance (mm)	Experimental test data for transient deformation, ' $\delta_T$ ' (mm)
A	3.75	200	54
B	8.75	200	107
C	8.75	130	165

## NUMERICAL SIMULATION

LS-DYNA, a numerical simulation software capable of performing explicit and implicit nonlinear analysis, developed by Livermore Software Technology Corporation, USA (LS-DYNA 2020) was utilized in this study to predict the maximum transient deformations of the RHA plates by using the LBE and the S-ALE methodologies. The following paragraphs will describe the steps to model the numerical simulation analysis of the blast loading of the RHA plate and will be presented in two different subsections for LBE and S-ALE, respectively.

### NUMERICAL SIMULATION: LOAD BLAST ENHANCED

Figure 5 shows the circular plate geometry to represent the physical RHA circular plate as used in the performed experimental test (see Figure 2 and Figure 3). 1 548 shell elements were used to construct the circular RHA plate that was 1 m in diameter. In the LBE methodology, the modeling of the spherical TNT was represented by a central point located above point B1 with the appropriate standoff distance. The mechanical properties utilized in the numerical simulation analysis are as listed in Table 1. The shell elements were of 20 mm in thickness, utilized Belytschko-Tsay shell element formulations, the number of through shell thickness integration points was '2' and Equation number '2' was utilized to represent the top surface of shell elements. In order to represent the clamping conditions of the RHA plate, whereby the circumference of the RHA plate was fully clamped as shown in Figure 3, a similar step was performed on the numerical simulation model i.e., the circumferential circular plate was fully fixed in the translational x, y, z and rotational rx, ry, rz directions. The 'control termination' of the model used was 30 ms to represent the complete blast loading scenario of the RHA plate, a 'timestep' of  $1.0 \text{ E-}5$  to capture the deformations of the blast loadings' events and a 'database\_ds3plot' of  $1.0\text{E-}05$  was used to record the animations of the blast loadings' deformations. The numerical simulation model was then submitted and processed in LS-DYNA (LS-DYNA 2020) by using Intel (R) Core (TM) i7-6820HQ CPU @ 2.70 GHz 2.70 GHz 16.0 GB, 64-bit operating system, x64-based processor hardware, an overall a time duration of around 30 minutes was utilized for each model.

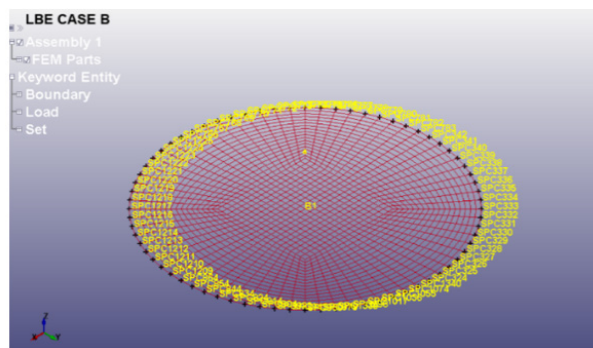


FIGURE 5. The geometry and elements constructions of the RHA plate in the numerical simulation utilizing the LBE methodology

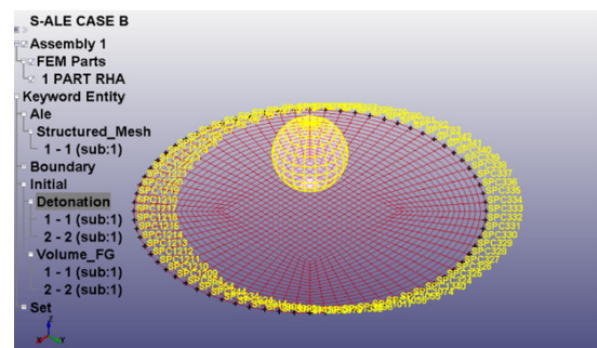


FIGURE 6. The circular geometry of the RHA plate and the spherical TNT bomb in the numerical simulation utilizing the S-ALE methodology

NUMERICAL SIMULATION: STRUCTURED ARBITRARY LANGRANGIAN EULERIAN

Figure 6 shows the circular plate representing the circular RHA plate as used in the experimental blast test (see Figure 2). The circular plate was made up of 1 548 shell elements with 1 m in diameter, one solid element of spherical TNT bomb and one solid set of three-dimensional cube of air elements. In the S-ALE methodology, there were three parts that had to be modelled i.e., the RHA plate (lagrangian), the spherical TNT (S-ALE), and the surrounding air (S-ALE) (see Figure 7). The spherical TNT bomb was placed above the central position of the circular RHA plate, both of these parts will be located inside a three-dimensional square element of air. Table 1 shows the mechanical properties of the circular RHA plate while the material properties and the equation of states for the air and TNT, respectively are as shown in Table 3. The circular RHA plate was fully fixed in the translational x, y, z and rotational rx, ry, rz directions to replicate the actual clamping scenario as observed during the performed experimental blast loading test. The ‘constrained lagrange in solid’ function was used to establish the S-ALE contact conditions between the RHA plate and the air and the RHA plate and the TNT bomb. The placement of all three parts i.e., shell elements of RHA plate, solid elements of TNT bomb, and solid elements of air were determined by using the ‘initial volume fraction geometry’ function whereby both the circular RHA plate and the spherical TNT bomb were placed and located at their respective coordinates inside the three-dimensional square air elements. Similar parameters of ‘control termination’, ‘timestep’, ‘database\_d3plot’, and computer hardware were used in the LBE analyses were also used in the S-ALE analyses to process the numerical simulation models and on average the processing time of each of the three analyses was around 80 minutes.

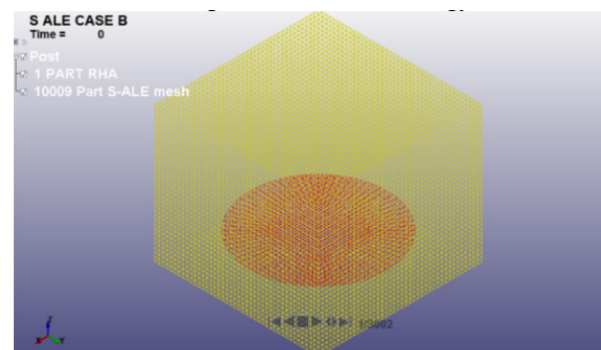


FIGURE 7. The circular geometry of the RHA plate and S-ALE three dimensional meshes of air in the numerical simulation utilizing the S-ALE methodology

TABLE 3. Material properties and equation of states for air and TNT

MAT_NULL			
Density=1.225 kg/m <sup>3</sup>			
EOS_LINEAR_POLYNOMIAL			
Air	C <sub>0</sub> =0	C <sub>1</sub> =0	C <sub>2</sub> =0
	C <sub>3</sub> =0	C <sub>4</sub> =0.4	C <sub>5</sub> =0.4
	C <sub>6</sub> =0	E <sub>0</sub> =253.4E3	
MAT_HIGH_EXPLOSIVE_BURN			
	Density=1630 kg/m <sup>3</sup>	D=6930 ms <sup>-1</sup>	PCJ=21.0E9 N/m <sup>2</sup>
TNT	EOS_JWL		
	A=371.20E9	B=3.231E9	R <sub>1</sub> =4.15
	R <sub>2</sub> =0.95	Omega=0.30	E <sub>0</sub> =7.0E9

Source: Dobratz & Crawford (1985)

## RESULTS AND DISCUSSION

The numerical simulation results consist of six sets of diagrams as shown in Figure 8 to Figure 19, each set consists of a diagram that describes the deformation patterns of the plate in the negative Z-axis direction (see Figure 8) and followed by the Z-axis displacement versus time graph (Figure 9) for Case A utilizing the LBE methodology for the first two figures and this order of presentation continues for the rest of the other five sets of numerical simulation analysis results in predicting the maximum transient deformations of the three experimental tests blast loadings data as conducted by Neuberger et al. (2009). Figure 8 shows the circular deformation patterns of the RHA plate due to the explosion of the spherical TNT bomb located at the central portion of the RHA plate. When a spherical TNT bomb explodes, the high pressure of explosive shockwaves travels outwards in a spherical expansion and away from the point source (Smith & Hetherington 1994), thus the circular deformation patterns that could be observed on the RHA plate are consistent with the very nature of the explosion behavior. Figure 9 shows the deformation histories of the central point of the RHA plate for a duration of 30 ms, when the shockwave of the explosion hits the central part of the RHA plate, the RHA deforms in the negative Z-direction reaching a maximum transient deformation magnitude of around -45.7 mm. This maximum transient deformation is the maximum amount of deformation experienced by the RHA plate and all six numerical simulation analysis predictions by using the LBE and S-ALE methodologies will be used to predict and compare against the maximum transient deformation values obtained from the performed experimental tests data (Neuberger et al. 2009).

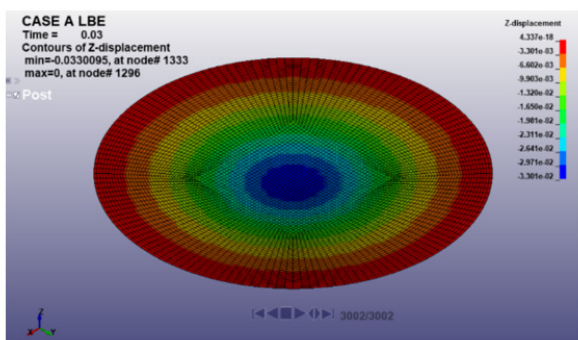


FIGURE 8. The Z-displacement patterns for Case A by utilizing the LBE methodology

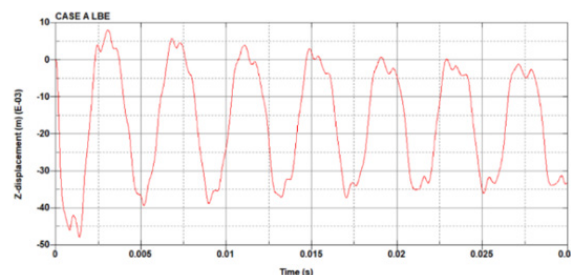


FIGURE 9. The Z-displacement vs time graph for Case A by utilizing the LBE methodology

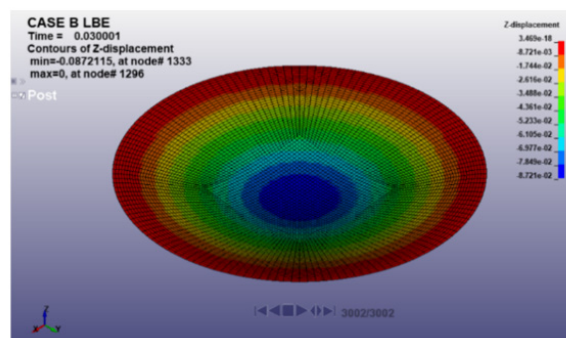


FIGURE 10. The Z-displacement patterns for Case B by utilizing the LBE methodology

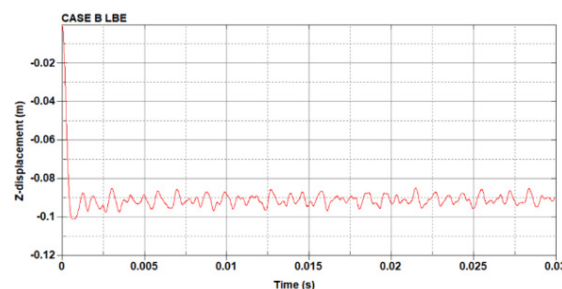


FIGURE 11. The Z-displacement vs time graph for Case B by utilizing the LBE methodology

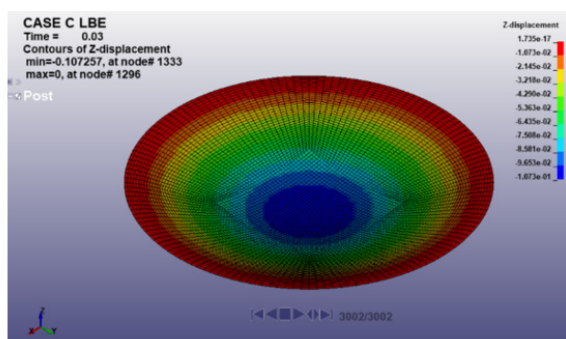


FIGURE 12. The Z-displacement patterns for Case C by utilizing the LBE methodology

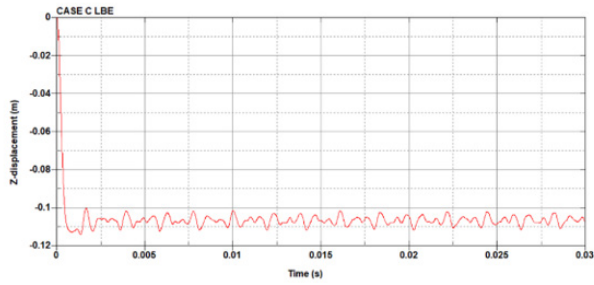


FIGURE 13. The Z-displacement vs time graph for Case C by utilizing the LBE methodology

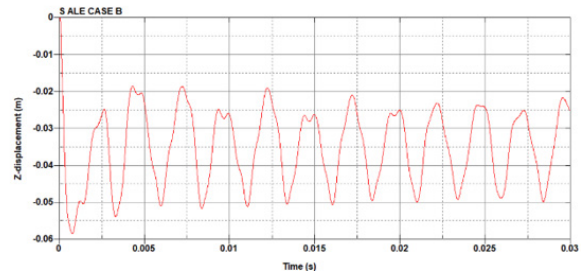


FIGURE 17. The Z-displacement vs time graph for Case B by utilizing the S-ALE methodology

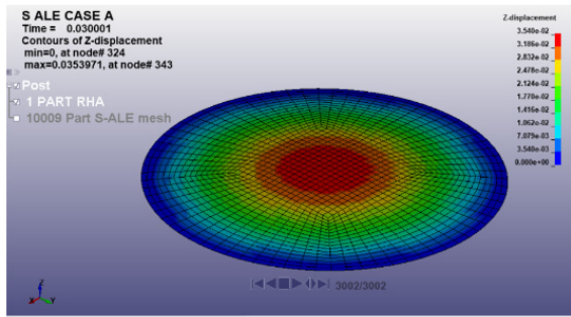


FIGURE 14. The Z-displacement patterns for Case A by utilizing the S-ALE methodology

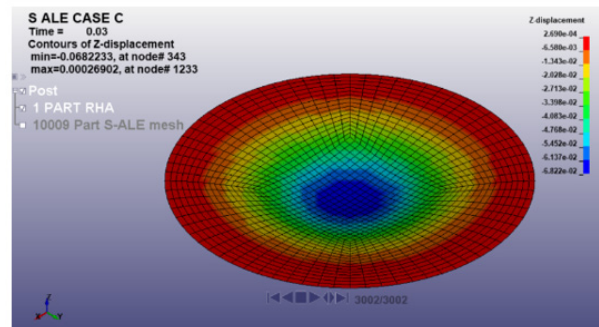


FIGURE 18. The Z-displacement patterns for Case C by utilizing the S-ALE methodology

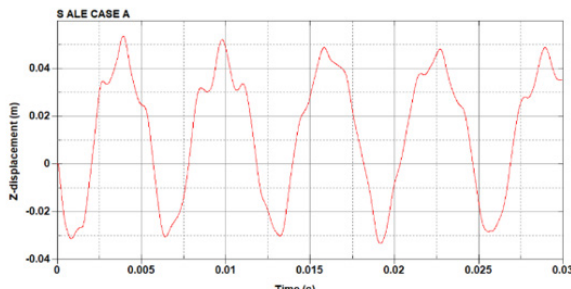


FIGURE 15. The Z-displacement vs time graph for Case A by utilizing the S-ALE methodology

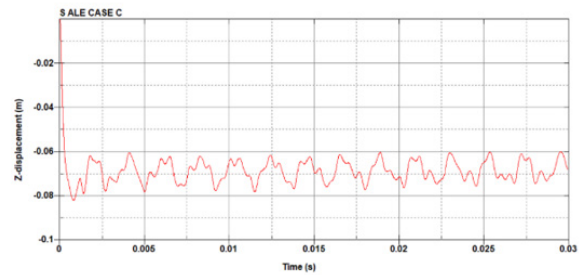


FIGURE 19. The Z-displacement vs time graph for Case C by utilizing the S-ALE methodology

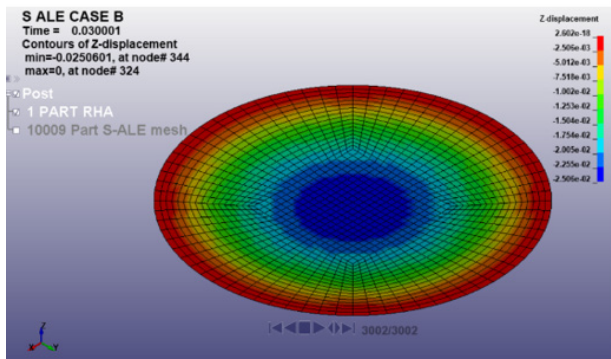


FIGURE 16. The Z-displacement patterns for Case B by utilizing the S-ALE methodology

Table 4 shows the complete numerical simulations results that utilized the LBE and S-ALE methodologies to predict the maximum transient central point deformations of the RHA plate obtained from the published experimental tests (Neuberger et al. 2009). Three maximum transient deformations results produced by the numerical simulations results that utilized LBE methodologies and three maximum transient deformations results produced by the numerical simulations results that utilized S-ALE methodologies had been produced and compared against the experimental data for Test Cases A, B and C with their respective percentage differences being calculated. Overall, it could be observed that the numerical simulations analysis that utilized LBE methodology gave good agreement with the experimental results as compared to the numerical simulations analysis that utilized S-ALE methodology,

where all of the three results from the S-ALE methodology underpredicts the experimental results by a factor of 2.

The LBE methodology is a simplified version of simulating blast loading scenarios in LS-DYNA whereby empirical pressure loads are applied directly to a 'langragian' structure and had a scaled distance validity from 0.05 m/kg<sup>1/3</sup> to 40 m/kg<sup>1/3</sup> and since the scaled distance of all three models constructed by using the LBE methodology in this study are within this range, thus it can produce good predictions. One factor that contributed to the differences between both numerical simulations methodologies and the experimental tests data was the application of boundary conditions of the numerical simulations models. Figure 2 and Figure 4 show the real physical scenario of the RHA clamped into the rigid test rig. It could be seen that the square RHA plate was clamped by two thick plates, six pair of bolts and nuts around the circumference of the circular RHA plate, and four square

pillars that rigidly fixed the RHA plate in its position throughout the experimental test. Unfortunately, Neuberger et al. (2009) did not specify the dimensions and locations detail of the bolts, nuts, and the four square pillars of the test rig, thus for this study, only the circular RHA plate of 1 m in diameter with 20 mm in thickness was modeled and was fixed around its circumference to closely represent the boundary conditions of the RHA plate being rigidly fixed during the experimental test (see Figure 5 and Figure 6). On the other hand, the S-ALE method is a 'relatively' new method introduced in LS-DYNA for the past few years. The set up of S-ALE related numerical simulations model is more complex than LBE and the processing time for S-ALE model takes longer to be solved. The coupling between the 'langrangian' part with the 'eulerian' part also had more parameters that had to be taken care of, thus making the predictions of S-ALE model less accurate.

TABLE 4. Final central deformation of rolled homogeneous armor steel plate due to TNT explosion; experimental (Neuberger et al. 2009) and numerical simulation comparisons

Test case	Weight of TNT (kg)	Standoff distance (mm)	Experimental test data for transient deformation (mm) (Neuberger et al., 2009)	LS-DYNA numerical simulation for transient deformation by using *Load Blast Enhanced (mm)	% Difference	LS-DYNA numerical simulation for transient deformation using *Structured Arbitrary Langrangian Eulerian (mm)	% Difference
A	3.75	200	200	45.7	-15.37	31.1	-42.40
B	8.75	200	200	101	-5.61	60.5	-43.45
C	8.75	130	130	115	-30.30	81.7	-50.48

## CONCLUSIONS

Two types of numerical simulations analysis utilizing the LBE and S-ALE methodologies have been presented in this study to predict the experimental tests data of three maximum transient deformations magnitudes of deformed circular surface area of RHA plate from a published paper (Neuberger et al. 2009). Results from the LBE methodology gave better agreement with respect to the published experimental tests data as compared to the S-ALE methodology because the LBE method is based on an empirical test data that could give reliable results even though it has workable range limits; conversely, the S-ALE method is more difficult to model and has a lot of complex parameters to deal with due to its coupling behavior.

## ACKNOWLEDGEMENTS

The authors would like to thank Mr Mohd Sharil bin Salleh from PPPI, UPNM for his kind assistance during the application process to obtain the short term grant and to the Management, Research and Innovation Center, National Defense University Malaysia (PPPI, UPNM) for the sponsorship of Short Term Research Grant (Grant number: UPNM/2019/GPJP/TK/4).

## DECLARATION OF COMPETING INTEREST

None

## REFERENCES

- Arief, N.P., Sigit, P.S., Leonardo, G., Djarot, W. & Ichsan, S..P. 2020. Numerical study and experimental validation of blastworthy structure using aluminum foam sandwich subjected to fragmented 8 kg TNT blast loading. *International Journal of Impact Engineering* 146: 103699.
- British Broadcasting Corporation. 2020. Beirut explosion: What we know so far. <https://www.bbc.com/news/world-middle-east-53668493>.
- Chao, H., Moubin, L., Bin, W. & Yuanping, Z. 2019. Underwater explosion of slender explosives: Directional effects of shock waves and structure responses. *International Journal of Impact Engineering* 130: 266-80.
- Chiquito, M., Castedo, R., Santos, A.P., López, L.M. & Pérez-Caldentey, A. 2020. Numerical modelling and experimental validation of the behaviour of brick masonry walls subjected to blast loading. *International Journal of Impact Engineering* 103760.
- Dobratz, B.M. & Crawford, P.C. 1985. LLNL explosives handbook - Properties of chemical explosives and explosive simulants, Technical Report UCRL 52997. In. Lawrence Livermore National Laboratory, University of California, CA, USA.
- Faucher, V., Casadei, F., Valsamos, G. & Larcher, M. 2019. High resolution adaptive framework for fast transient fluid-structure interaction with interfaces and structural failure – Application to failing tanks under impact. *International Journal of Impact Engineering* 127: 62-85.
- Gannon, L. 2019. Submerged aluminum cylinder response to close-proximity underwater explosions – A comparison of experiment and simulation. *International Journal of Impact Engineering* 133: 103339.
- Hailing, Y. & David, Y.J. 2016. Impact dynamics and puncture failure of pressurized tank cars with fluid–structure interaction: A multiphase modeling approach. *International Journal of Impact Engineering* 90: 12-25.
- Hughes, K., Vignjevic, R., Campbell, J., Vuyst, T.De., Djordjevic, N. & Papagiannis, L. 2013. From aerospace to offshore: Bridging the numerical simulation gaps–Simulation advancements for fluid structure interaction problems. *International Journal of Impact Engineering* 61: 48-63.
- Wu, Y.L. Peng & Q. Fang. 2020. Experimental and numerical study of ultra-high performance cementitious composites filled steel tube (UHPCCFST) subjected to close-range explosion. *International Journal of Impact Engineering* 141: 103569.
- LS-DYNA. 2020. [www.lstc.com](http://www.lstc.com).
- Neuberger, A., Peles, S. & Rittel, D. 2009. Springback of circular clamped armor steel plates subjected to spherical air-blast loading. *International Journal of Impact Engineering* 36: 53-60.
- Qinghua, Q., Yuanming, X., Jianfeng, L., Shangjun, C., Wei, Z., Kaikai, L. & Jianxun, Z. 2020. On dynamic crushing behavior of honeycomb-like hierarchical structures with perforated walls: Experimental and numerical investigations. *International Journal of Impact Engineering* 145: 103674.
- Q. Su, H. Wu, H.S. Sun & Q. Fang. 2021. Experimental and numerical studies on dynamic behavior of reinforced UHPC panel under medium-range explosions. *International Journal of Impact Engineering* 148: 103761.
- Smith, P.D. & Hetherington, J.G. 1994. *Blast and Ballistic Loading of Structures*. Oxford: Butterworth-Heinemann Ltd.
- Spinosa, E. & Iafrati, S. 2021. Experimental investigation of the fluid-structure interaction during the water impact of thin aluminium plates at high horizontal speed. *International Journal of Impact Engineering* 147: 103673.
- Vinh-Tan, N. & Gatzhammer, B. 2015. A fluid structure interactions partitioned approach for simulations of explosive impacts on deformable structures. *International Journal of Impact Engineering* 80: 65-75.
- Wei, Z., Guang-yan, H., Han, L., Wei, L., Xiao-bin, B. & Shun-shan, F. 2020. Experimental and numerical investigation of a hollow cylindrical water-based barrier against internal blast induced fragment loading. *International Journal of Impact Engineering* 138: 103503.
- Xiangzhen, K., Qin, F., Jinhua, Z. & Yadong, Z. 2020. Numerical prediction of dynamic tensile failure in concrete by a corrected strain-rate dependent nonlocal material model. *International Journal of Impact Engineering* 137: 103445.
- Ying, L., Zhaoyue, C., Xianben, R., Ran, T., Ruxin, G. & Daining, F. 2020. Experimental and numerical study on damage mode of RC slabs under combined blast and fragment loading. *International Journal of Impact Engineering* 142: 103579.
- Y. Yuan, P.J. Tan, K.A. Shojaei & Wrobel, P. 2017. The influence of deformation limits on fluid–structure interactions in underwater blasts. *International Journal of Impact Engineering* 101: 9-23.